Estuarine, Coastal and Shelf Science 134 (2013) 57–68

Contents lists available at ScienceDirect

Estuarine, Coastal and Shelf Science

journal homepage: www.elsevier.com/locate/ecss

Impact of coral spawning on the biogeochemistry of a Hawaiian reef

R.A. Briggs [a,*,1], J.L. Padilla-Gamiño [a,b,1,2], R.R. Bidigare [b], R.D. Gates [b], K.C. Ruttenberg [a]

[a] Department of Oceanography, University of Hawai'i, 1000 Pope Rd., Honolulu, HI 96822, USA
[b] Hawai'i Institute of Marine Biology, University of Hawai'i, PO Box 1346, Kane'ohe, HI 96744, USA

ARTICLE INFO

Article history:
Received 5 March 2013
Accepted 17 September 2013
Available online 2 October 2013

Keywords:
coral
spawning
nutrients
biogeochemistry
Montipora capitata

ABSTRACT

We examined the impact of *Montipora capitata* coral spawning on local biogeochemistry in Kane'ohe Bay, Hawai'i. This event supplied labile, spawn-derived organic matter (SDOM) to the water column, triggering a cascading series of related effects on the biogeochemistry of the reef. Specifically, we measured the isotopic composition and nutrient ratios of spawning material and coral tissues, and utilized these signatures to track pathways of SDOM incorporation into this coral-dominated ecosystem. We observed: (1) shifts in the isotopic signatures of coral tissues after the spawning event, (2) rapid turnover of SDOM within the water column and enhanced deposition of POM to the sediment surface, (3) enhanced sediment efflux of NH_4^+ after the spawning event that triggered a phytoplankton bloom in the overlying water, and (4) drawdown of dissolved nutrients in the water column after spawning that coincided with the occurrence of a water column phytoplankton bloom. Our results show that single-species spawning events can serve as a source of substantial nutrient input to the water column, contributing in similar ways to storm-driven river nutrient input, and with measurable impact on the biogeochemistry of the reef.

1. Introduction

Coral reefs are characterized by exceedingly high rates of productivity and biodiversity, yet are typically situated in nutrient-poor (oligotrophic) waters (e.g., Furnas et al., 2005). Consequently, perturbations in the quantity of bioavailable essential nutrients can influence coral growth and physiology, and affect the population dynamics and community composition of coral reefs (Szmant, 2002). It is important to understand the biogeochemical processes that supply nutrients to these systems, as the nature of these processes and the magnitude of their impact on essential nutrient inventories will affect the productivity and biodiversity of coral reef ecosystems.

Most corals are hermaphroditic broadcast spawners that release bundles containing buoyant lipid-rich eggs and sperm (Baird et al., 2009). Coral spawning events occur over a short period (min–hr) and can result in the influx of large quantities of labile organic material into the reef system. It is well documented that episodic inputs of labile organic matter to coastal waters (i.e. storm events) impact dissolved inorganic and organic nutrient concentrations and ratios. Changes in the nutrient regime can shift phytoplankton community composition, selecting for certain phytoplankton over others. To better understand the impact of spawning material on water column biogeochemistry, the concentration of essential nutrients (nitrogen (N) and phosphorus (P) and carbon (C)) in labile organic material released during spawning must be quantified. Examining the organic C:N:P ratio in coral tissue and spawn material also provides insight into coral condition, as they are essential bioelements, and their relative proportions reflect the abundance of important biomolecules such as lipids, carbohydrates and proteins (Bodin et al., 2007).

Nutrient release from spawn derived organic matter (SDOM) to the water column has the potential to significantly influence trophic interactions (Westneat and Resing, 1988; Baird et al., 2001; Pratchett et al., 2001), biogeochemical processes in oligotrophic reef systems (Eyre et al., 2008; Glud et al., 2008; Wild et al., 2008), and in rare occasions can cause extensive mortality of corals and other reef animals (Simpson et al., 1993). Eggs that are not fertilized in the water column have several potential fates, including (1) abiotic or biotic decomposition within the water column, (2) direct sedimentation, and (3) ingestion by organisms within the water column and subsequent sinking of fecal matter to bottom sediments (Wild et al., 2004a, 2008). The use of elemental ratios and

* Corresponding author.
E-mail addresses: briggs@hawaii.edu (R.A. Briggs), gamino@lifesci.ucsb.edu (J.L. Padilla-Gamiño).
[1] Authors contributed equally to this work.
[2] Current address: Ecology, Evolution and Marine Biology, University of California Santa Barbara, Santa Barbara, CA 93106-6150, USA.

0272-7714/$ – see front matter © 2013 Elsevier Ltd. All rights reserved.
http://dx.doi.org/10.1016/j.ecss.2013.09.013

isotopic composition of spawn material, water column particulates, and sediments can assist in our understanding of these pathways. Molar organic carbon to total nitrogen to organic phosphorus ratios (OC:TN:OP) and carbon isotopic values are the principle tools for distinguishing sources of organic matter (e.g., Hedges and Parker, 1976; as cited by Goni, 1997; Ruttenberg and Goñi 1997a, b). Additionally, shifts in the $\delta^{15}N$ value of water column particulates can be used to examine food web dynamics, because $\delta^{15}N$ values are enriched by an average of 3.4 ± 1.1 per mil with each trophic level (reviewed in Maier et al., 2010).

Previous studies examining the biogeochemical response to mass coral spawning at the Great Barrier Reef (GBR) found that nutrient regeneration from mineralized SDOM in both the water column and sediments can trigger a chain of pelagic and benthic processes which significantly influence nutrient recycling and the reef community within these systems (Eyre et al., 2008; Glud et al., 2008; Wild et al., 2008). Even a small spawning event at the GBR was shown to increase sedimentary oxygen consumption rates for up to nine days after spawning and played a role in the nutrition of microbial communities in the benthos (Wild et al., 2004b). Increased primary production (water and sediments) was documented several days following a large spawning event in the GBR, presumably fueled by nutrients released by the mineralization of SDOM (Glud et al., 2008; Wild et al., 2008).

To date, the effects of coral spawning on reef biogeochemistry have only been documented at the GBR, where multi-species spawning events, involving over 130 species, occur (Willis et al., 1985; Harrison and Wallace, 1990). Additional research is needed, however, to examine and compare the responses to spawning in other regions where coral species do not spawn synchronously and/or there are fewer species participating in the event (Guest, 2008). This study explores, for the first time, the influence of a single-species coral spawning event on the nutrient dynamics of a coral reef system located in the Central Pacific (Hawai'i). We examined how SDOM produced by *Montipora capitata* spawning events in Kane'ohe Bay, Hawai'i alter nutrient budgets and influence water column primary production. *Montipora capitata* is one of the most abundant and important reef building coral species in the main Hawaiian Islands (Jokiel et al., 2004), and is a hermaphroditic broadcast-spawner that releases egg-sperm bundles to the water column for external fertilization during the new moon of summer months (Hodgson, 1985; Hunter, 1988; Kolinski and Cox, 2003).

The guiding hypothesis of this study was that *Montipora capitata* coral spawning events in Kane'ohe Bay supply a quantity of labile, spawn-derived organic matter (SDOM) to the water column that has a cascading series of related effects on the biogeochemistry of the system. First, we considered that the elemental and isotopic composition of water column particulate matter would be altered due to the input of SDOM, and that this signature might also be visible in surface sediments that would receive sinking SDOM. Second, we anticipated that water column dissolved nutrient inventories would be enhanced due to rapid mineralization of the labile pool of SDOM, and that this in turn could trigger a water column phytoplankton bloom.

2. Methods

2.1. Study site

This study was conducted at Gilligan's Lagoon (21° 25.973'N; 157° 47.392'W) on the western side of Moku O Lo'e Island (Coconut Island) in Kane'ohe Bay (O'ahu, Hawai'i). Gilligan's Lagoon is a semi-enclosed area with fringing reefs comprised mostly of *Montipora capitata* and *Porites rus* coral species.

2.2. Environmental conditions

A multi-parameter YSI 6600V2 Sonde® and a LiCor 193 Spherical Quantum Sensor® were deployed within 2 m of the sampling location to monitor real-time water conditions during the spawning event in 2008. The YSI Sonde measured temperature, salinity, turbidity, conductivity, pH, and pressure (depth). The LiCor sensor measured photosynthetically active radiation (PAR), and was adapted with a small cup on the lower side of the spherical sensor to avoid reflective radiation from the sediment water interface. A bottom-mounted 600 kHz RD Instruments acoustic Doppler current profiler (ADCP)® was placed in the lagoon to monitor water motion throughout the study. The instrument measures flow in 3 directions, u (north and south), v (east and west), and w (vertical motion). Flow data in each direction was used to create a current velocity vector plot from 2.12 m above the seabed, with positive-y vectors in the northern direction. To compare site characteristics between the study years (2007–2008), environmental measurements (temperature, precipitation, wind, solar and ultraviolet (UV) radiation) were taken at meteorological stations at the Hawai'i Institute of Marine Biology on Moku O Lo'e Island. Temperature was recorded using a Campbell Scientific temperature probe (model 107), precipitation was recorded using a Texas Electronics Tipping bucket rain gauge (Eppley, TE525), wind was recorded with a R.M. Young Wind Monitor (Young, 05103), sun-plus-sky radiation was measured using a silicon pyranometer with 0.2 kW m^{-2} mV^{-1} sensitivity (Campbell Scientific, L1200X-L), and UVR was measured using a total ultraviolet radiometer with 8 $\mu V/Wm^{-2}$ sensitivity (EPLAB, TUVR). All environmental variables were recorded hourly.

2.3. Coral tissue and spawn material collection and analysis

Tissue samples from the same adult coral colonies were collected before (pre-) and after (post-) spawning during 2007 and 2008 (pre-spawn: 9 June 2007 and 27 May 2008; post-spawn: 30 September 2007 and 21 September 2008). Sampling periods were chosen to ensure that we collected before and after the major spawning events. *Montipora capitata* is a partial spawner (individuals can spawn over consecutive nights or consecutive lunar months) with most spawning occurring from June to August (Padilla-Gamiño and Gates, 2012). Coral tissue samples were collected by breaking a small fragment of the parental colony from regions where polyps were anticipated to be reproductively active (at least 4 cm away from tips and edges: Wallace, 1985). Samples were placed immediately on dry ice and stored at −80 °C until further analysis.

Gametes were collected upon release into the water column during the spawning events of summer 2007 and 2008 from colonies located in ~1–2 m of water. The gametes were collected on the fringing reef using a novel net system that caused minimal damage to both adult coral colonies and released gametes (Padilla-Gamiño and Gates, 2012). The cylindrical nets were placed on coral colonies 1–2 h before spawning commenced and were removed every night after completion of the spawning event. The collected egg-sperm bundles were rinsed with filtered (0.2 μm Pall Life-Sciences® polycarbonate) seawater (FSW) and aliquots placed immediately in Costech® aluminum capsules for carbon and nitrogen analysis. An additional aliquot of egg-sperm bundles was rinsed with FSW to break apart the bundles and isolate sperm packets from eggs. Sperm packets were placed in Costech® aluminum capsules for elemental (C and N) analysis and eggs were placed in Eppendorf® tubes. Egg-sperm bundles, eggs, and sperm samples were stored at −80 °C until analyzed.

All elemental, isotopic and biochemical measurements were obtained using samples that included coral and endosymbiont

tissue (except for sperm samples that do not contain endosymbionts). Coral fragments were ground using mortar and pestle and homogenized in FSW using a Polytron homogenizer (PT 2100, Kinematica). Skeleton was removed from the homogenate using multiple centrifuge steps with several FSW washes. The remaining sample (coral tissue) was filtered onto pre-combusted 25 mm glass fiber filters (Whatman® GF/F, 0.7 μm nominal pore size) for organic carbon (OC) and total nitrogen (TN) analysis.

Eggs collected during spawning were also filtered onto pre-combusted GF/F filters for analysis. Adult coral tissue material on GF/F filters was acidified to remove inorganic carbon (IC) by slowly adding 3 N HCl, drop wise, to each filter and drying at 60 °C after acidification was complete. Coral tissue and egg samples on GF/F filters, as well as aluminum capsules that were prepared in the field with whole bundle and sperm samples, were analyzed for carbon and nitrogen concentrations and isotopic values at the Isotope Biogeochemistry Laboratory at the University of Hawaii, Manoa. Carbon and nitrogen isotopic values are reported using conventional δ-notation with respect to VPDB and atmospheric N_2, respectively. Total phosphorus in eggs and coral tissue was determined using a high-temperature ashing/hydrolysis method (Aspila et al., 1976), and analyzed spectrophotometrically via the molybdenum blue method (Grasshoff et al., 1983); phosphorus content of whole bundle and sperm samples was not determined. Inorganic phosphorus content of corals and eggs was below detectable levels, and thus we report total phosphorus only, which is equivalent to organic phosphorus (OP) in this data set. All filtered samples were normalized to total ash-free dry coral tissue biomass of the organic fraction, according to Grottoli et al. (2004), to account for residual skeleton material. Ash free dry weight (AFDW) represents the mass of the organic portion of the sample, and is calculated by subtracting the mass of the ash (inorganic content only) from the total mass (inorganic + organic content) of the sample. Total lipids were extracted from coral fragments according to Rodrigues and Grottoli (2007). In brief, lipids were extracted from ground samples (skeleton + coral tissue) in a 2:1 chloroform/methanol solution. The organic phase was washed using 0.88% KCl and the extract dried to a constant weight. Triacylglycerol (TAG) and wax ester (WE) concentrations in total lipid extracts were determined by high-performance liquid chromatography/evaporative light-scattering detection (HPLC/ELSD) using triolein (Sigma–Aldrich, #1787-1AMP) and oleyl oleate (Sigma–Aldrich, #O3380) as reference standards (Silversand and Haux, 1997). For pigment analysis, GF/Fs containing the coral and algal tissue homogenate were extracted in 3 mL of HPLC-grade acetone with 50 μL of an internal standard (canthaxanthin) at 4 °C in the dark for 24 h. The extracts were processed according to Bidigare et al. (2005). To estimate symbiont density, *Symbiodinium* cells were separated from the tissue homogenate by performing multiple centrifugation and washing steps using FSW. After separation, the *Symbiodinium* pellets were resuspended in FSW and homogenized, and three subsamples were enumerated manually with a hemocytometer and a light microscope (Olympus BX-51).

2.4. Water and sediment sample collection and analysis

Water and sediment samples were collected pre-, post-, and during spawning in June 2008 over a 19-day time period. Samples collected pre- and post-spawn event were collected at noon (12:00) and midnight (00:00). On the three days over which spawning occurred (3–5 June 2008), samples were collected at noon (00:00), at the start of bundle release (~21:00), at the end of bundle release (~22:00), and 1.5 h after spawning ceased (~23:30). Surface and bottom water samples were collected at each time point in acid-washed, sample-rinsed 1-L HDPE bottles and immediately transferred to shore for filtration. Water samples were also collected for pigment analysis using a soap-washed and sample rinsed 250-mL amber bottles. Small sediment push cores were collected at each sampling time point from a sediment patch surrounded by coral heads using a modified 60-cc syringe as a coring device.

Sediment push cores were sectioned into 3 intervals (0–2 cm, 2–4 cm and 4–6 cm) under an inert (N_2) atmosphere to prevent oxidation artifacts (Bray et al., 1973). Porewater was separated from bulk sediment via centrifugation. In order to maximize porewater collection, Whatman VectaSpin 20® centrifuge tubes were adapted to allow filtration during centrifugation by replacing the manufactured installed polypropylene filter with a coarse 24 mm glass fiber filter (VWR® Grade 696, 1.2 μm nominal pore size). The coarse glass fiber filter allowed maximum recovery of sediment porewater from sandy sediment, which was subsequently filtered using 0.4 μm Pall Life Sciences GHP acrodisc® filters. Filtered porewater was split into two subsamples: a frozen, untreated split and a refrigerated-acidified split, analyzed for ammonium (NH_4^+) and dissolved phosphate (PO_4^{3-}), respectively, using well-established colorimetric protocols (Grasshoff et al., 1983) on a BioTek Synergy HT Multi-Mode Microplate Reader. The microplate reader permits colorimetric detection on small porewater sample volumes (300-μL), allowing for the analysis of multiple dissolved constituents on a single porewater interval, despite the small volumes of porewater collected from each interval. We used Nunc 96-well Optical Bottom Plates®, which have a 1-cm path length, comparable to that of standard spectrophotometric detection. Total dissolved phosphorus (TDP) was determined on porewaters using a modified high-temperature ashing-hydrolysis method and analyzed via the molybdenum blue method; dissolved organic phosphorus (DOP) is calculated as the difference between TDP and dissolved inorganic phosphorus (PO_4^{3-}) (Monaghan and Ruttenberg, 1999). All reported colorimetric data have a 2% standard error associated with them. Porewater concentrations of PO_4^{3-} and NH_4^+ are the focus of this paper; other data are available upon request.

After removal of porewater, sectioned sediment intervals were frozen under an inert atmosphere until freeze-dried under vacuum to prevent oxidation artifacts (Krall et al., 2009). Sediments were ground with an agate mortar and pestle, sieved (<125 μm) and stored in sealed vessels prior to analysis. Sediment inorganic phosphorus (IP) was determined utilizing acid hydrolysis, and sediment total phosphorus (TP) was determined using high-temperature ashing/hydrolysis; OP was calculated as the difference between TP and IP (Aspila et al., 1976). Total carbon (TC), OC, IC and TN, as well as carbon and nitrogen isotope values ($\delta^{13}C$ and $\delta^{15}N$, respectively), were determined on sediments using a combined coulometric (IC)-elemental analyzer-mass spectrometry method, in which OC is quantified as the difference between TC and IC (OC = TC-IC). Carbon and nitrogen isotopic values are reported using the conventional δ-notation as described in Section 2.4.

A 700-mL split of surface and bottom water collected in the 1L HDPE bottles was filtered through a pre-weighed 47-mm polycarbonate filter (Whatman®, 0.2 μm nominal pore size), which was acid-washed and rinsed with MQ-H_2O prior to use. Filtrate was split into two subsamples: a frozen, untreated split and a refrigerated-acidified sample. Frozen, untreated splits were analyzed for dissolved PO_4^{3-}, $Si(OH)_4$, NO_3^-, NO_2^-, NH_4^+, total dissolved nitrogen (TDN), and total dissolved phosphorus (TDP) on a Technicon AutoAnalyzer II® following well-established analytical methods at The Water Center at the University of Washington. DOP and dissolved organic nitrogen (DON) were determined as the difference between TDP and TDN and the dissolved inorganic P and N pools.

A 250-mL split of the remaining sample water was filtered through pre-combusted 25 mm GF/F filter for the analysis of particulate OC

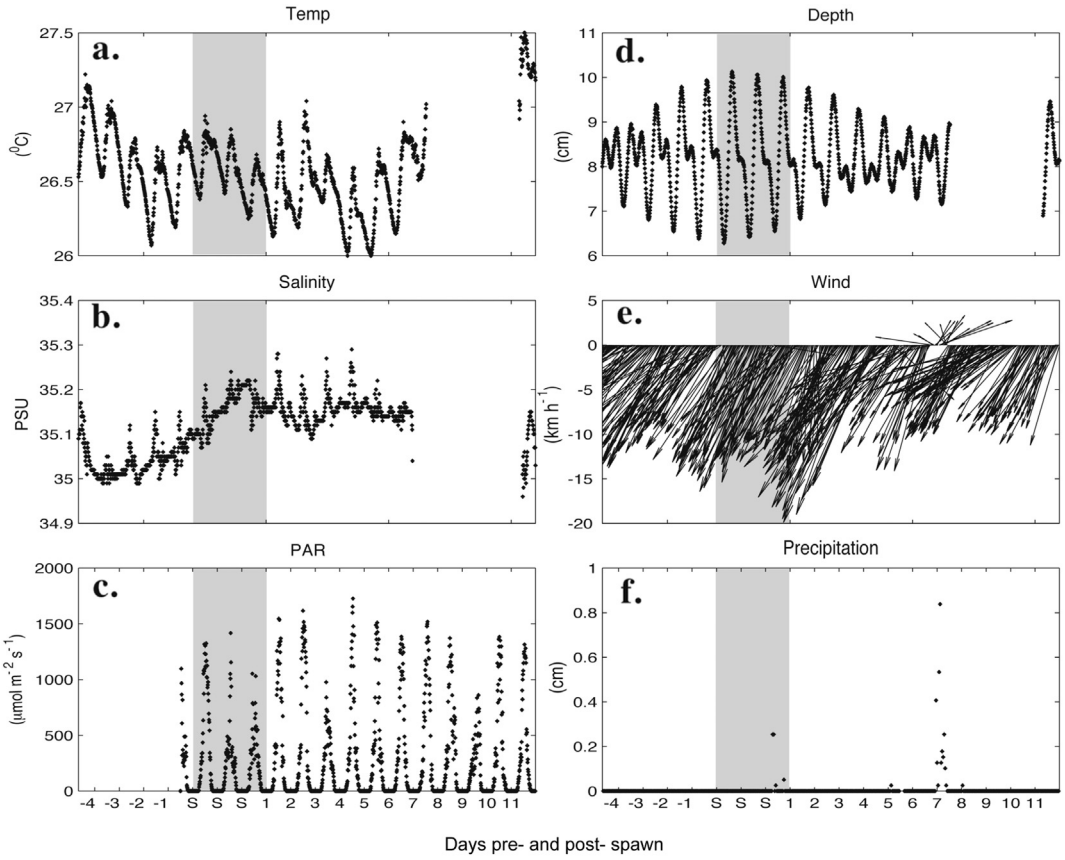

Fig. 1. *In situ* instruments were deployed within 2 m of the sampling location to monitor water quality in real-time throughout the study during the 2008 spawning event. A multi-parameter YSI 6600V2 Sonde® provided data on (a) temperature (°C), (b) salinity (practical salinity units) and (d) water depth (cm), and a LiCor 193 Spherical Quantum Sensor® provided data on (c) PAR (µmol m^{-2} s^{-1}). Additionally, (e) wind speed and direction (km h^{-1}; positive-y is the north direction), as well as (f) precipitation (cm) data were obtained from the Hawai'i Institute of Marine Biology (HIMB) weather station. Dates are reported as days pre- (negative) or post- (positive) spawning, with the three consecutive days of spawning marked as three consecutive 'S' on the *x*-axis and shaded in the plot.

and TN, as well as carbon and nitrogen isotope values ($\delta^{13}C$ an $\delta^{15}N$, respectively). Filters were acidified and analyzed according to the procedures described previously for host tissue samples.

Sample water collected in the amber bottles was filtered through a 25 mm GF/F filter to collect suspended particulates for photosynthetic pigment analysis. Filtered particulate samples were frozen at −80 °C prior to analysis. Samples were extracted and analyzed by reverse-phase high-performance liquid chromatography (HPLC) as described by Bidigare et al. (2005).

3. Calculations

3.1. Benthic nutrient efflux calculations

Sediment porewater profiles were used to calculate diffusive nutrient fluxes across the sediment–water interface using Fick's first law of diffusion. Fluxes were calculated based upon the difference between the peak concentration of porewater NH_4^+ and PO_4^{3-} within the top 6 cm below the sediment–water interface and the NH_4^+ and PO_4^{3-} concentration in the overlying bottom water, respectively. The whole molecular diffusion constants for seawater were based on values from Boudreau (1997) ($NH_4^+ = 1.85 \times 10^{-9}$ and $PO_4^{3-} = 8.9 \times 10^{-10}$, respectively). Sediment tortuosity as calculated from the porosity of sediments using the assumptions outlined in Boudreau (1997). Calculated diffusive fluxes do not include advective processes, and thus represent minimum porewater flux estimates.

3.2. Statistical analysis

Prior to statistical analysis, data were normalized as necessary using logarithmic transformation to achieve homogeneity of variances and normality. Data were analyzed using a general linear model, with year, pre/post-spawning and colony as fixed factors. Colony was nested within the pre/post-spawning category to account for the repeated measurements between periods before and after spawning (Sokal and Rohlf, 1994). Means, standard deviations and ranges (minimum–maximum) of temperature and light were calculated for each site during the periods sampled. Temperature and light measurements were compared between years and sites using a Mann Whitney test. *p*-values were considered significant below an alpha of 0.05.

4. Results

4.1. Environmental conditions

Spawning of *Montipora capitata* occurred during the first quarter of the new moon in June, July and August of 2007 and 2008. Spawning took place over three consecutive days each month between the hours of 20:45 and 21:15.

In June 2008, when the biogeochemical sampling occurred, average water temperature and salinity (± standard error from daytime fluctuations) were 26.6 ± 0.3 °C and 35.1 ± 0.1 psu, respectively (Fig. 1a–b), and diurnal variations in PAR were

observed with peak values of 1726 μmol m^{-2} s^{-1} (Fig. 1c). YSI pressure sensor data revealed semi-diurnal tidal fluctuations, with spring tide conditions during spawning events (Fig. 1d). Trade-wind conditions, characterized by an absence of rainfall and NE winds at 10–20 km h^{-1}, persisted throughout the study (Fig. 1e), with the exception of a small rain event and wind shift that occurred 7 days after spawning ceased (Fig. 1e and f). This rain event was brief (8 h), and peaked at 03:00 on the morning of June 12, resulting in 0.84 cm of rain (Fig. 1f). The ADCP data reveal extremely low and variable flow rates (<5 ± 2 cm s^{-1}), which register just above the detection limit of the instrument (Fig. 2). In general, water elevation was tidally driven (represented by the dark trend line; units plotted on left-hand *y*-axis in Fig. 2a–c). Horizontal currents were slow and variable, yielding a velocity vector plot that clearly indicates the absence of uni-directional flow during tidal shifts (Fig. 2d). For specific details of the environmental characteristics and spawning dynamics between the 2007 and 2008 see Padilla-Gamiño and Gates (2012).

4.2. Coral and spawn material

Sample size differed among the analyses (n = 11–13 for coral tissue samples, n = 4–15 gamete samples). The average OC:OP ratio from 2007 and 2008 pre- and post-spawn coral tissue samples (n = 12) was 364 ± 18. Significant changes in OC:OP ratios were not observed between spawning years or between pre- and post-spawn samples (p = 0.759, p = 0.814, Fig. 3a, Table 1). $\delta^{13}C$ values were heavier in the post-spawning samples than the pre-spawning coral tissue samples (p = 0.001, Fig. 3, Table 1). The average $\delta^{13}C$ values in pre- and post-spawn coral tissue samples (both years) were −13.3 ± 0.4 and −12.2 ± 0.4, respectively (Fig. 3, Table 1). Overall, $\delta^{13}C$ values were heavier in 2008 than 2007 (p = 0.001, Table 1) and substantial variability within colonies was observed (p = 0.001, Table 1).

Bundle (n = 10) and sperm (n = 4) material $\delta^{13}C$ values were similar to host tissue samples with $\delta^{13}C$ values of −12.1 ± 0.1 and −13.0 ± 0.1 respectively. However, eggs (n = 15) displayed a $\delta^{13}C$ value of −14.5 ± 0.1, lighter than either sperm or bundles (Fig. 3b). The average OC:TN ratios in pre-spawn host tissue samples from both years were not significantly different from OC:TN ratios of post-spawn coral tissues; the average OC:TN ratio of all coral tissues was 11.0 ± 0.4. Bundle, egg, and sperm material had OC:TN ratios of 19.1 ± 0.5, 21.4 ± 0.6, and 5.3 ± 0.1, respectively, all of which are significantly different from coral host tissues (F = 140.98, df = 3, p < 0.0001, Fig. 3b). Spawned bundles displayed $\delta^{15}N$ values that averaged 4.6 ± 0.1 (n = 10), and the mean OC:TN:OP (C:N:P) ratio of coral egg material from spawning events in our study site was 838:35:1 (n = 6) (data not shown). Overall, OC:TN was lower in coral tissues from 2007 than 2008 (p = 0.038, Table 1).

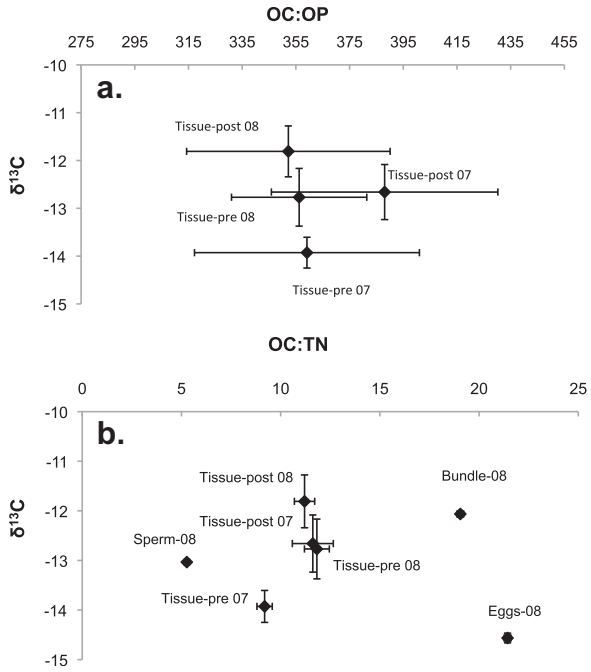

Fig. 3. Isotopic signatures and nutrient ratios of gamete and adult coral tissues from 2007 to 2008: (a) OC:OP versus $\delta^{13}C$ for coral tissue; (b) OC:TN versus $\delta^{13}C$ for coral tissue, egg, sperm, and bundles. Error bars represent standard errors associated with replicate sample analysis (coral tissue n = 12; bundles n = 10; eggs n = 15; sperm n = 4).

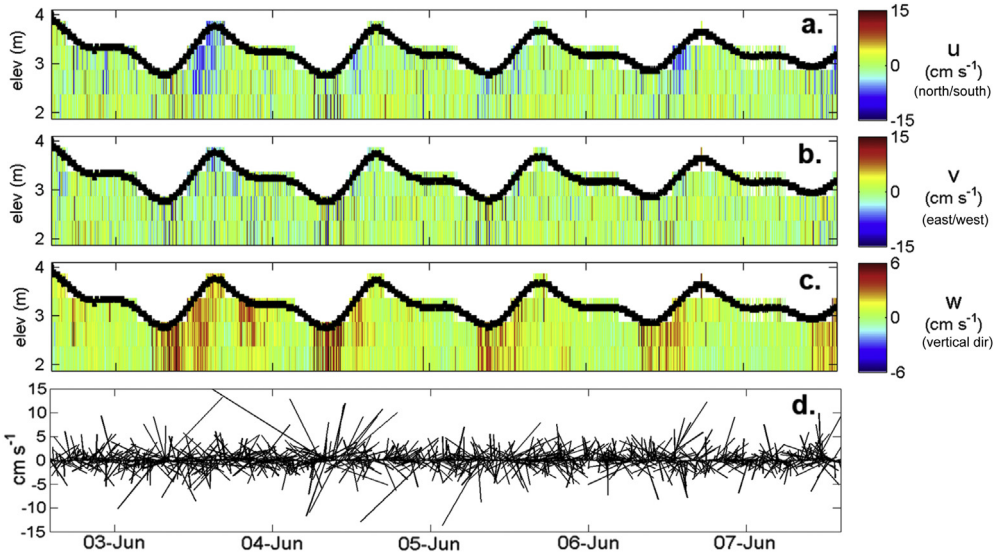

Fig. 2. Data from a 600 kHz RD acoustic doppler current profiler deployed in Gillian's lagoon for five days during the 2008 spawning event. Water velocity (cm s^{-1}) is displayed on the right-hand *y*-axis in three directions: (a) north/south: u, (b) east/west: v, and (c) vertical motion: w. Water elevation (m) is on the left-hand *y*-axis and is displayed as a dark black line on each panel. Panel (d) displays the horizontal currents from 2.12 m above the seafloor as current velocity vectors, where positive-y is the northeast direction.

Table 1
Results of the general linear model testing the effects of year, pre/post spawning and colony on $\delta^{13}C$, OC:OP, OC:TN, Lipid, WE and TAG content, Chl *a* concentration and *Symbiodinium* densities of *Montipora capitata*. df = degrees of freedom, F = F-statistic, p = p-value. Significant values at 95% confidence ($p < 0.05$) are in bold.

Variable	df	Effect of year		Effect of pre/post		Effect of colony (pre/post)		Effect of year* pre/post	
		F	p	F	p	F	p	F	p
$\delta^{13}C$	46	13.57	**0.001**	16.19	**0.001**	4.50	**0.001**	1.06	0.314
OC:OP	46	0.10	0.759	0.06	0.814	0.71	0.781	0.46	0.506
OC:TN	46	4.89	**0.038**	2.25	0.148	1.23	0.317	5.91	**0.024**
Lipids	51	1.31	0.263	8.85	**0.007**	0.77	0.390	1.82	0.075
WE	51	6.86	**0.015**	15.24	**0.001**	6.00	**0.022**	2.06	**0.042**
TAG	51	2.29	0.143	0.10	0.756	0.41	0.526	1.12	0.390
Chl *a*	47	3.76	0.065	0.28	0.602	0.08	0.780	2.79	0.010
Symb. densities	43	0.58	0.455	0.08	0.777	0.62	0.441	1.43	0.217

Lipid content and wax esters (WE) were higher in pre-spawning coral tissues than post-spawning tissues ($p = 0.007$, $p = 0.001$, respectively, $n = 13$, Table 1,Fig. 4a,b) and overall WE were higher in the year 2008 than 2007 ($p = 0.015$, respectively, $n = 13$, Table 1,Fig. 4b). Colony had a significant effect on WE concentrations before and after spawning, indicating that there is a large variation in WE concentrations between colonies ($p = 0.022$, Table 1). Triacylglycerols (TAG) ($n = 13$), Chl *a* ($n = 12$) and *Symbiodinium* densities ($n = 11$) did not show significant differences between pre- and post-spawning coral samples or between years (Fig. 4c–e).

4.3. Water column and sediment data

$\delta^{13}C$ values of surface water particles prior to spawning were lighter (-19.4 ± 0.6; $n = 6$) than samples collected 24 h after spawning commenced (-13.6 ± 0.8; $n = 3$) (Fig. 5a); bottom water column particles displayed a similar trend towards heavier $\delta^{13}C$ values immediately following spawning. $\delta^{15}N$ values in water column particulates from surface and bottom waters were heavier during- and post-spawn (7.5 ± 0.3; $n = 38$) compared to pre-spawn values of 4.9 ± 0.4 ($n = 12$) (Fig. 5b). Sediments and water column particulates were characterized by OC concentrations ranging from 0.5 to 3.5 wt % (Fig. 5c), with water column particulate OC concentrations higher than bottom sediments. OC and TN concentrations and OC:TN ratios of water column particulates and surface sediments post-spawn were not different from pre-spawn sample OC and TN concentrations and ratios (Fig. 5c–e).

Diffusive flux calculations show positive fluxes of NH_4^+ and PO_4^{3-} to the overlying water at all sampling times (Fig. 6). While the magnitude of the PO_4^{3-} flux was relatively invariant during the study period (0.78 ± 0.36 μmol m^{-2} d^{-1}), within 24 h after the last spawning event, benthic ammonium fluxes were nearly 4-fold higher than pre-spawn fluxes, with a maximum flux of 39 μmol m^{-2} d^{-1} on the first day after spawning ceased (Fig. 6).

Prior to the first night of spawning Chl *a* levels in surface and bottom waters were relatively invariant (316 ± 38 ng L^{-1}). Six days after the spawning event Chl *a* levels increased by 3 times over the concentration observed during the pre-spawn period (Fig. 7a). Fucoxanthin, a biomarker pigment for diatoms, spiked to 288 ng L^{-1} synchronously with Chl *a* (Fig. 7b). A total of 52 particulate water column samples were collected for Chl *a* and photosynthetic pigment analysis. Because our intent was to use Chl *a* as a marker for water column phytoplankton biomass response to SDOM-derived nutrients, we excluded 4 high Chl *a* samples from the data set that also had exceedingly high concentrations of peridinin, the pigment characteristic of dinoflagellates. These high peridinin values (30–130 times background levels) most likely indicate the presence of the dinoflagellate endosymbionts present in the eggs of the bundles (*Montipora capitata* has vertical transmission of symbionts), and do not reflect free-living phytoplankton biomass.

Overall, dissolved inorganic and organic nutrient concentrations from surface and bottom waters were relatively similar (Fig. 8), indicating a well-mixed water column during most of the study. Prior to the first night of spawning, water column concentrations of NH_4^+ and PO_4^{3-} averaged 0.42 ± 0.11 μmol L^{-1} (Fig. 8a) and 0.16 ± 0.02 μmol L^{-1} (Fig. 8b), respectively. After the spawning event had run its course, NH_4^+ and PO_4^{3-} concentrations decreased to near detection limits (0.92 and 0.07 μmol L^{-1}, respectively). $Si(OH)_4$ concentrations were ~8 μmol L^{-1} at the start of the study and steadily decreased after spawning commenced to a low of ~2 μmol L^{-1} by day 12 post-spawn (Fig. 8c). To confirm that this decrease was not an artifact of instrument drift, these samples were re-run manually on the BioTek Plate reader (see Section 2.4) using a colorimetric molybdenum-blue method (Grasshoff et al., 1976). Values obtained on the plate reader were within 5% of values reported from the auto-analyzer at the Water Resource Center, and displayed the same decreasing trend (data not shown). Pre-spawn NO_2^- + NO_3^- (NO_x) averaged 0.21 ± 0.09 μmol L^{-1} ($n = 12$) (Fig. 8d); NO_x concentrations increased 2-fold after the spawning event.

DON concentrations increased slightly after spawning commenced (pre-spawn: 6.8 ± 0.3 μmol L^{-1}; post-spawn: 8.0 ± 0.3 μmol L^{-1}); DOP concentrations were invariant during the study period (pre-spawn: 0.2 ± 0.01 μmol L^{-1}; post-spawn: 0.2 ± 0.01 μmol L^{-1}) (Fig. 8e and f). Two samples collected during the spawning event (spawning days 1 and 2) that display high levels of DON and DOP likely reflect sampling artifacts, as samples collected 30 min later did not present similarly high levels of DON or DOP (Fig. 8e and f). We suspect that bundles caught on the filter may have broken apart during filtration, artificially elevating the levels of dissolved organic nutrients in these two samples. Dissolved inorganic nitrogen (DIN = NO_x + NH_4^+) to dissolved inorganic phosphorus (DIP = PO_4^{3-}) ratios increased after the last day of spawning (Fig. 8g) from average DIN:DIP (mol mol^{-1}) in pre-spawn samples of 4.0 ± 0.3 ($n = 12$) to a post-spawn maximum of 15. DON:DOP (mol mol^{-1}) ratios were essentially invariant, with an average value of 39.8 ± 0.7 ($n = 52$) throughout this study (Fig. 8h).

5. Discussion

5.1. Characterization of coral tissue and spawn material

Coral tissues after the reproductive season (post spawning) were enriched in ^{13}C when compared to coral tissues prior to the reproductive season and to spawned eggs (Fig. 3). This finding could be attributed to (1) changes in the biochemical characteristics of tissues of the coral colony before and after the reproductive

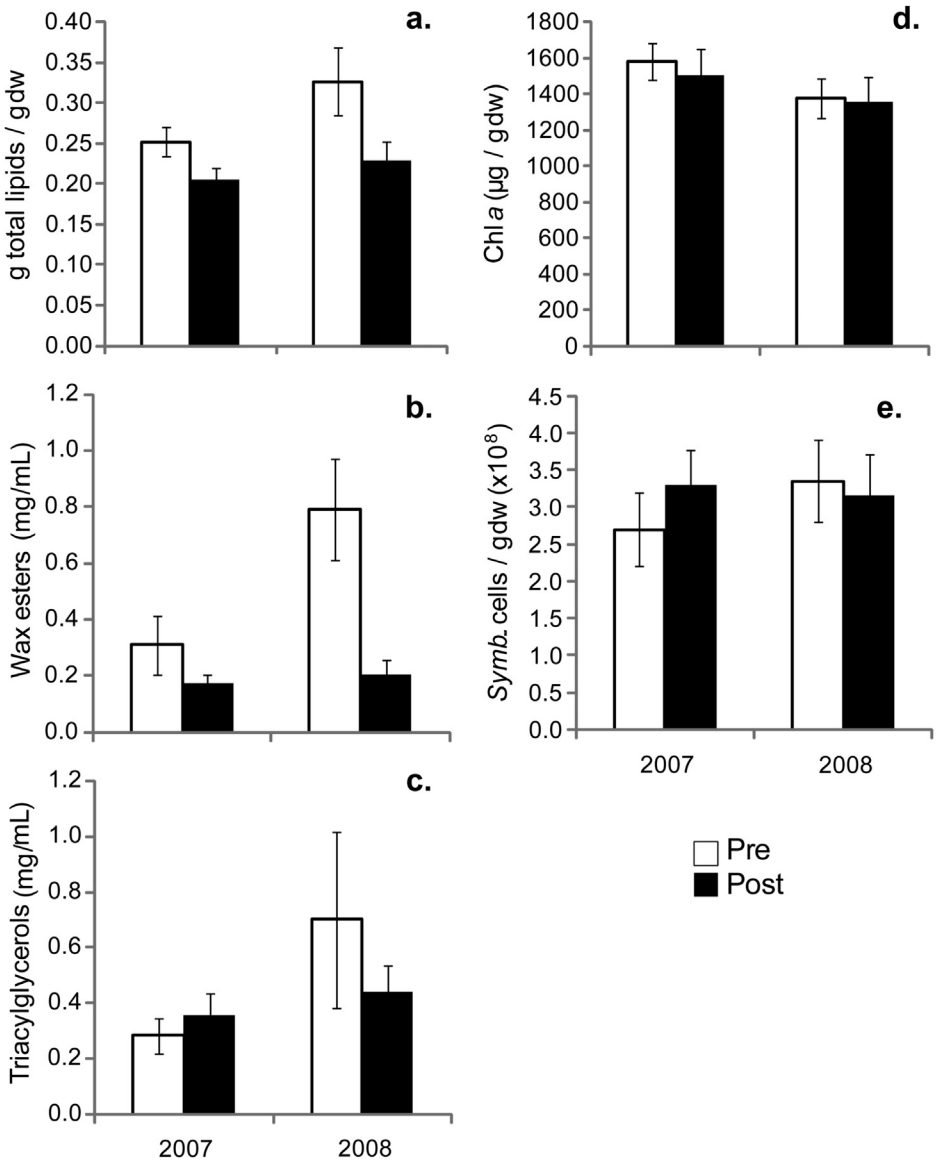

Fig. 4. Traits investigated in coral tissue of *Montipora capitata*, before and after the spawning season in 2007 and 2008. (a) Lipid (g total lipids/gdw), (b) WE (mg/mL), (c) TAG (mg/mL), (d) Chl *a* (µg/gdw) and (e) *Symbiodinium* densities (Symb cells/gdw $\times 10^8$). Error bars represent standard errors associated with replicate sample analysis ($n = 13$ for lipids, WE and TAG, $n = 12$ for Chl *a* and $n = 11$ for *Symbiodinium* densities for pre- and post-spawning samples collected in both years).

season (June–September), (2) the result of a decrease in heterotrophic feeding habits, and/or an increase in autotrophy (Grottoli and Wellington, 1999; Rodrigues and Grottoli, 2006; Alamaru et al., 2009a), (3) or both. Our results support the first scenario since coral adults have a higher lipid content (in the form of wax esters) at the beginning of the reproductive season (Fig. 4a and b), and the lipid composition differs between pre- and post-spawning tissues (Fig. 4b and c). At the end of the reproductive season, coral host tissues display diminished WE concentrations relative to pre-spawn levels. Because WE are a major component in *Montipora capitata* eggs (Padilla-Gamiño et al. 2013), loss of eggs during spawning could explain the diminished WE content of host tissue after the spawning season. In contrast to WE, Triacylglycerol (TAG) concentrations do not change between pre- and post-spawning samples, suggesting that the relative proportion of TAG in coral tissue increases in post-spawn samples. It has been suggested that storage lipids such as TAG are isotopically enriched relative to other lipid classes (Grottoli and Rodrigues, 2011), and it is possible that the higher $\delta^{13}C$ signatures observed post-spawn are driven by an increase in the relative proportion of TAG in the coral tissue. The second scenario (changes in heterotrophic/autotrophic carbon acquisition) seems less likely, since Chl *a* and *Symbiodinium* densities did not change before and after the reproductive season.

The OC:TN ratio of coral egg material determined in this study (21:1) is slightly higher than previously reported values for coral eggs (~18:1) (Wild et al., 2004b). The OC:OP ratio, however, is substantially higher (838:1) than previously reported values (316:1) (Eyre et al., 2008). Differences in elemental ratios may be attributed to differences in the spawning material characteristics at each location. In particular, *Montipora capitata* eggs contain dinoflagellate endosymbionts, whereas the majority of spawning material collected by Eyre et al. (2008) was most likely asymbiotic, as most spawning coral species do not transmit symbionts via the egg (Baird et al., 2009). As carbon is a principal structural component in dinoflagellates (Menden-Deuer and Lessard, 2000), and symbiont densities inside *Montipora capitata* eggs are estimated to range

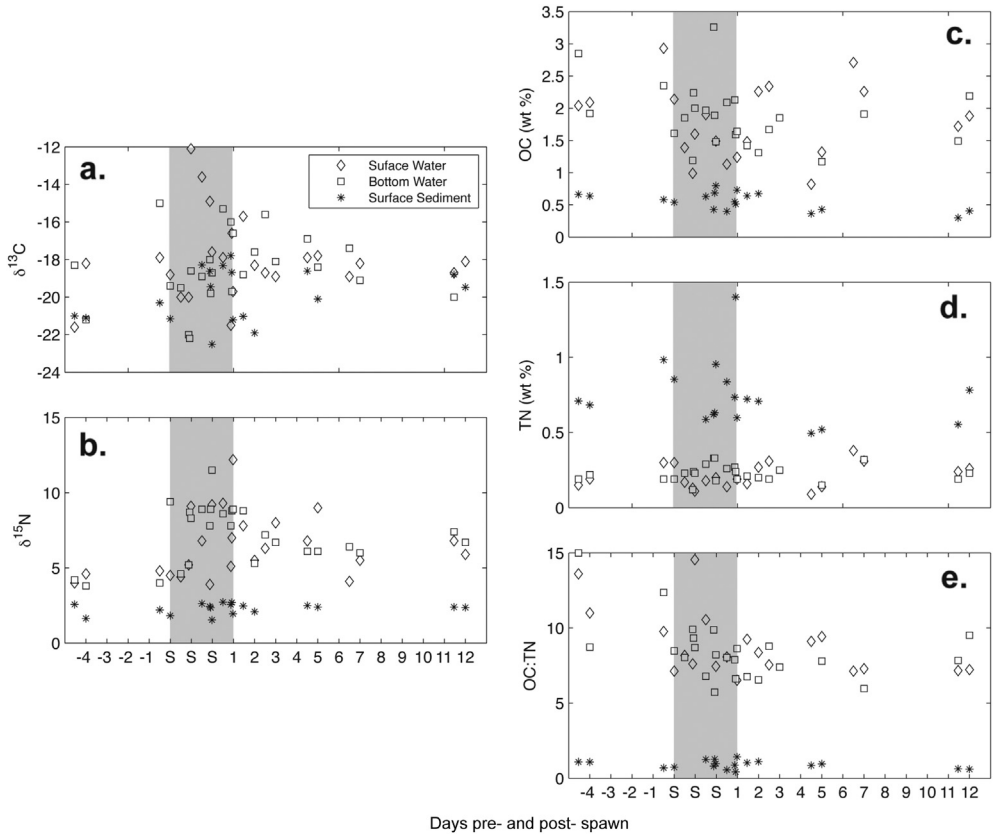

Fig. 5. (a) $\delta^{13}C$ isotopic values, (b) $\delta^{15}N$ isotopic values, (c) OC concentrations (wt percent), (d) TN concentrations (wt percent), and (e) OC:TN ratio of surface (diamonds) and bottom water (squares) particulate samples and surface sediments (stars). Dates are reported as days pre- (negative) or post- (positive) spawning, with the three consecutive days of spawning marked as three consecutive 'S' on the *x*-axis and shaded in the plot. Isotopic signatures that display perturbations due to the spawning event are circled.

between 2.4 and 4.2 $\times$ 10^3 cells per egg (Padilla-Gamiño et al., 2013), the endosymbiont component of the spawn material characterized in our study could contribute greatly to the higher OC:TN ratios we observe relative to other studies. Another caveat important to consider in comparing the elemental ratios in our study with other published data is that we separated the coral eggs from the bulk spawn material, and thus our values only represent coral eggs. Eyre et al. (2008) sampled the bulk spawn slick, which would have contained a mixture of material, including eggs, sperm, bundle material, and possibly extraneous materials not directly associated with the spawning event.

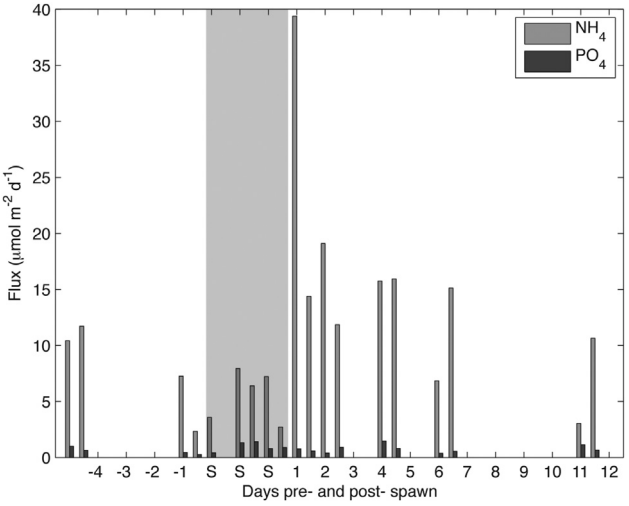

Fig. 6. Calculated benthic diffusive fluxes of NH_4^+ (light gray) and PO_4^{3-}(black). Nutrient fluxes across the sediment water interface were calculated from sediment porewater profiles using Fick's first law of diffusion. Dates are reported as days pre- (negative) or post- (positive) spawning, with the three consecutive days of spawning marked as three consecutive 'S' on the *x*-axis and shaded in the plot.

The OC:TN values of individual spawn components (eggs, sperm) were strikingly different than the whole bundle from which they were derived (Fig. 3b). A simple mass balance calculation, assuming that the bundle is comprised entirely of eggs and sperm and using the measured OC:TN ratios of these components, suggests that the bundle is comprised of 85% eggs and 15% sperm. This is consistent with our understanding of the structure of the bundle (Padilla-Gamiño et al., 2011). However, the $\delta^{13}C$ values of egg and sperm components cannot be explained using these relative percentages (Fig. 3b), because the bundle is characterized by a heavier $\delta^{13}C$ value than each of the individual components (sperm and egg) alone, suggesting that there is another source of heavy carbon in the bundle that is unrelated to the gametes. The most likely sources of this heavier carbon are *Symbiodinium* cells attached on the surface of the bundle or between the eggs, and/or packaging material within the bundle, which consists of a mucus layer possibly secreted by the oocytes (Padilla-Gamiño et al., 2011).

5.2. Tracking the impact of SDOM on water column suspended particulate and surface sediment organic matter

The $\delta^{13}C$ signature of surface water particulates (Fig. 5a) displays a clear and pronounced perturbation due to the spawning event. Carbon isotopic values of surface water particulates for 24 h

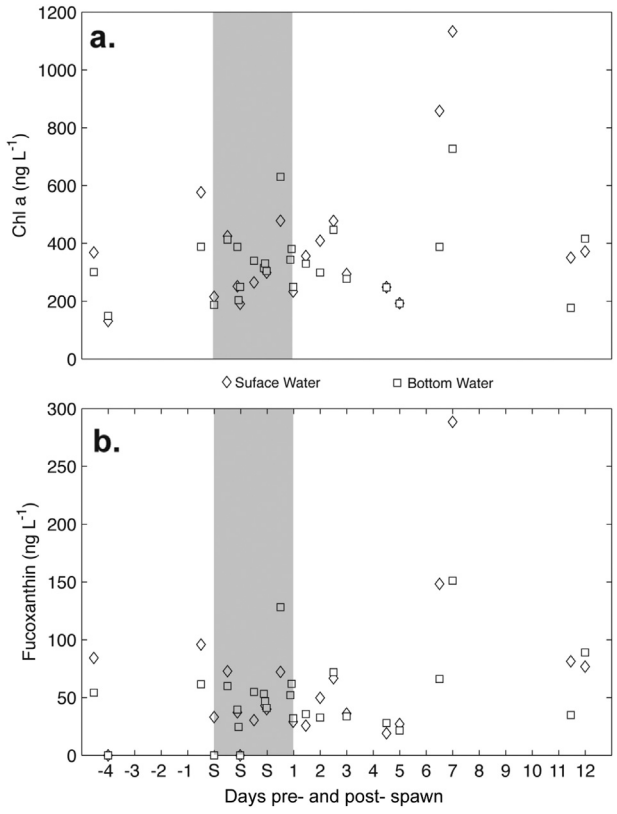

Fig. 7. Photosynthetic pigment data from water column particulates: (a) Chl *a* (ng L^{-1}) and (b) fucoxanthin (ng L^{-1}) concentrations from surface (diamonds) and bottom (squares) waters. Dates are reported as days pre- (negative) or post- (positive) spawning, with the three consecutive days of spawning marked as three consecutive 'S' on the *x*-axis and shaded in the plot.

following the onset of spawning were enriched by ~6 per mil over pre-spawn values, reflective of the inclusion of spawn material in the water column particulate pool (Figs. 3b and 5a). Particulates collected from bottom water also display post-spawn enrichment, but the effect lags the perturbation seen in surface water particles by 1–2 days. Variability in $\delta^{13}C$ is substantially more muted in surface sediments than in water column particulates, but nonetheless an enrichment of 2 per mil is detectable in surface sediments by day-2 of the spawn event (Fig. 5a). A similar impact on $\delta^{15}N$ is observed in surface and bottom water particulates (enrichment of 7 and 6 per mil, respectively), but no effect is discernable in surface sediments (Fig. 5b).

Post-spawn, water column particulate $\delta^{13}C$ values trend relatively rapidly back to background values, while $\delta^{15}N$ values remain at enriched levels relative to pre-spawn values (Fig. 5a and b). The $\delta^{15}N$ value of water column particulates can be used to examine food web dynamics, because $\delta^{15}N$ values are enriched by an average of 3.4 ± 1.1 per mil with each trophic level (reviewed in Maier et al., 2010). The $\delta^{15}N$ enrichment over pre-spawn values we observe in water column particulates (Fig. 5b) reflects the cumulative effect on the isotopic composition of water column particulates as higher trophic levels feed on SDOM (Fry, 1988).

While the incorporation of SDOM into the ecosystem is apparent when examining the isotopic values of water column particulates, the impact of SDOM on bulk OC concentrations of both water column particulates and surface sediments is less evident (Fig. 5c). There is no discernible difference in OC concentrations pre- to post-spawn in either water column particulates or surface sediments (Fig. 5c). We attribute the absence of a post-spawn increase in sediment OC concentration to the dilution effect by non-organic sedimentary material. The high inorganic carbon (i.e. $CaCO_3$) in the sediments makes it difficult to observe differences in OC concentrations pre- and post-spawn, as OC is determined using a difference method (OC = TC-IC; see Section 2.4).

TN concentrations are higher in surface sediments than in water column particulates (Fig. 5d), which is the inverse of the observed distribution of OC between water column particulates and surface sediments. The observed N-enrichment in surface sediments can be explained by microbial colonization of deposited organic matter, as bacteria are enriched in N relative to C (Rice and Hanson, 1984). The depressed OC:TN ratios in surface sediments (Fig. 5e) are consistent with bacterial enrichment of surface sediments in TN over water column particulates. We interpret the absence of a discernible trend in OC:TN pre- to post-spawn as indicative of the fact that the degree of microbial colonization on SDOM is equivalent to that on sediment organic matter not associated with SDOM.

Highly permeable reef sands act as biocatalytic particle filter systems in which coral-derived organic matter (including SDOM) decomposes rapidly upon deposition (Wild et al., 2005, 2008; Glud et al., 2008). SDOM deposited on the seabed can have a profound impact upon the system through the rapid regeneration of inorganic nutrients from this labile organic matter pool. The post-spawn benthic diffusive flux of NH_4^+ is nearly 4 times that of pre-spawn effluxes the day after the spawning event (Fig. 6). The observed NH_4^+ fluxes in this study are an order of magnitude lower than those estimated for Kane'ohe Bay (490 μmol m^{-2} d^{-1}, Stimson and Larned, 2000). This discrepancy can be reconciled if we consider that (1) only the top 6 cm of the sediment was sampled in this study, whereas peak porewater concentrations were observed at a depth of ~50 cm in Kane'ohe Bay sediments (Stimson and Larned, 2000), and (2) fluxes calculated in this study only take into account diffusive processes; advective processes would increase the estimated benthic fluxes. While the fluxes calculated in this study may underestimate the expected true flux values, they are nevertheless useful for examining relative changes in benthic nutrient efflux over the spawning period, and can be used to interpret the ecosystem response to SDOM deposition.

Increased porewater NH_4^+ efflux persisted for several days after spawning, reflecting the time period over which labile SDOM was being decomposed in sediments. Previous studies have verified the significant role of sediments in recycling SDOM, and have observed enhanced benthic NH_4^+ efflux following mass spawning events as well as enhanced sediment oxygen consumption (Wild et al., 2004b; Eyre et al., 2008). The fact that no enhancement of benthic PO_4^{3-} efflux was observed in our study can be attributed to the highly particle reactive nature of PO_4^{3-}, and indicates probable sediment sequestration of porewater PO_4^{3-} liberated by SDOM remineralization in the seabed (Fig. 6).

Despite the large benthic efflux of porewater NH_4^+ (Fig. 6), dissolved water column inventories of NH_4^+ decreased following the spawning event (Fig. 8a). Removal of NH_4^+ from the water column can be accomplished by a number of processes, including (1) physical flushing of nutrients out of the lagoon, (2) biological uptake, and/or (3) nitrification in the water column. The low flow rates observed in Gilligan's Lagoon during the study period, and the absence of any systematic flow direction (Fig. 2), imply that minimal physical flushing of nutrients out of Gilligan's Lagoon occurred during the study. Thus, physical removal of NH_4^+ via flushing of the lagoon is not likely. However, the low flushing rates set up conditions ideal for accumulation of phytoplankton biomass in the water column, including bloom initiation, and for prolonging growth without disruption. During this period of increased growth, biological uptake of nutrients supplied by enhanced sediment efflux can occur.

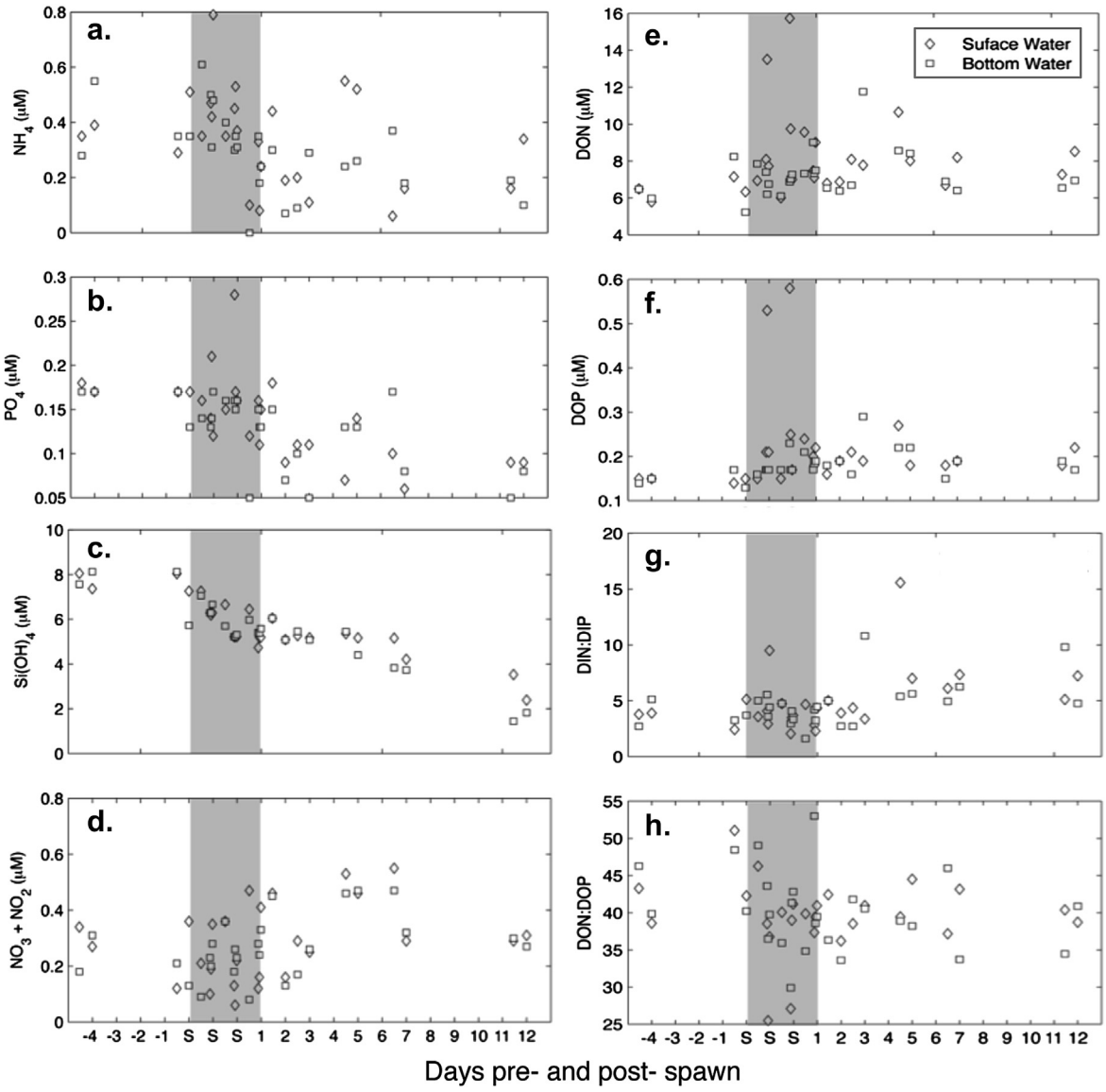

Fig. 8. Dissolved nutrient concentrations (µmol L^{-1}) and nutrient ratios of surface water (diamonds) and bottom water (squares): (a) NH_4^+ (b) PO_4^{3-} (c) $Si(OH)_4$ (d) $NO_x = NO_2^- + NO_3^-$ (e) DON (f) DOP (g) DIN:DIP and (h) DON:DOP. Dates are reported as days pre- (negative) or post- (positive) spawning, with the three consecutive days of spawning marked as three consecutive 'S' on the *x*-axis and shaded in the plot.

As shown in Fig. 7 enhanced phytoplankton biomass was observed six days after the last *Montipora capitata* spawning day in June 2008 at Gilligan's Lagoon, as evident by the 3-fold increase in both Chl *a* and fucoxanthin concentrations in water column particulates. The rapid production of Chl *a,* and the short duration of elevated Chl *a* concentrations in the water column (Fig. 7a) is characteristic of the boom-bust sequence described in other systems that receive episodic nutrient input (Ringuet and Mackenzie, 2005; Eyre and Ferguson, 2006). In a boom-bust sequence, water column primary productivity rapidly increases due to an enhanced, short-term supply of nutrients. The bloom quickly collapses as nutrients are consumed and drop to limiting levels. In our study, we first observed the bloom at noon (12:00) on 11 June 2008. Because of a 2-day sampling gap that occurred prior to 11 June, it is possible that the bloom initiated 1–2 days prior to June 11, which would mean that the bloom could have persisted for 3–4 days, rather than the 1–2 days that our Chl *a* and fucoxanthin data suggest (Fig. 7).

The bloom event observed in this study was similar in size and duration to storm-enhanced primary production that has been documented in other studies (Ringuet and Mackenzie, 2005; Eyre and Ferguson, 2006), suggesting that increases in water column nutrients associated with spawning events may stimulate boom-bust water column production sequences similar to those observed with episodic fluvial inputs of nutrients. Precipitation during our study was light (Fig. 2f), and the single rain event that occurred during our study happened after the Chl *a* concentrations peaked (Fig. 7). Thus, we can confidently rule out storm-derived nutrients as the trigger for the bloom we observed in the post-spawn period of our study.

The phytoplankton bloom observed post-spawn resulted in substantial drawdown of water column NH_4^+ and PO_4^{3-}, and an even more pronounced drawdown of $Si(OH)_4$ (Fig. 8a–c). We attribute the removal of $Si(OH)_4$ to uptake by diatoms, which dominated the bloom as evidenced by the coincident increase in fucoxanthin and Chl *a* in water column particulates (Fig. 7). In

contrast to NH_4^+ and PO_4^{3-}, which were drawn down post-spawn, water column NO_x concentrations increased after the spawning event (Fig. 8d). We explain the observed increase in water column NO_x as a consequence of water column nitrification fueled by the enhanced benthic efflux of NH_4^+ observed post-spawn. Enhanced benthic NO_x flux could also contribute to the post-spawn water column concentrations, as has been observed to occur in the GBR (Eyre et al., 2008), but NO_x flux was not constrained as part of this study. The increase in DIN:DIP ratios observed post-spawn (Fig. 8g) is driven both by the increase in water column NO_x (Fig. 8d) and the decrease in water column PO_4^{3-} (Fig. 8b). Elevated levels of DON and DOP in surface waters on the first 2 days of the spawning event could be due either to excretion by the phytoplankton that comprise the bloom, and/or by sloppy feeding or excretion by zooplankton feeding on the blooming phytoplankton.

Gilligan's Lagoon is characterized by DIN:DIP ratios well below the canonical Redfield ratio (16:1, N:P), with an increase in DIN:DIP ratios (primarily driven by increased NO_x concentrations) observed after spawning (Fig. 8g). Recognizing that the Redfield ratio is not necessarily a universal optimum for phytoplankton growth (Arrigo, 2005), it does provide a metric for examining nutrient limitation in an ecosystem (e.g., Healey and Hendzel, 1980; Hecky and Kilham, 1988). Oligotrophic waters surrounding coral reef ecosystems are characterized by low, often limiting nutrient concentrations (e.g., Furnas et al., 2005). Kane'ohe Bay has been described as an N-limited environment during non-storm conditions (Laws and Allen, 1996; Ringuet and Mackenzie, 2005), and the DIN:DIP ratios observed in this study are consistent with the notion of an N-limited system. The post-spawn increase in DIN:DIP suggests, however, that the post-spawn bloom draws down DIP at more rapid rates than DIN, potentially shifting the system towards conditions in which phytoplankton could become P-stressed. This aligns well with reports by Ringuet and Mackenzie (2005) who noted shifts towards P limitation following episodic inputs of storm-derived nutrients to Kane'ohe Bay.

Substantial differences exist in the post-spawn behavior of water column nutrients in the GBR (Eyre et al., 2008), as contrasted with our study site in Kane'ohe Bay. In the GBR, DIN was almost completely removed from the water column post-spawn, while DIP inventories were only minimally drawn down. Dissolved organic forms of N and P were important to benthic and pelagic production in GBR coral reef systems, whereas in this study the changes in the DON and DOP pool were insignificant, and therefore are considered to provide only minor sources of nutrients for the observed biomass increase (Fig. 8e and f). These observed differences in water column inorganic and organic nutrient inventories following spawning events highlight the regional variations in nutrient recycling patterns that can occur in systems that are subject to episodic nutrient input as a consequence of coral spawning events.

Apprill and Rappè (2011) studied the microbial community response during a coral spawning event near our study site, and observed no change in Chl *a* after a spawning event. These authors suggested that no biogeochemical response was imparted to the ecosystem by the release of gametes from the spawning coral, which at face value is in direct contradiction to the observations made in our study. We can reconcile this discrepancy if we consider the important differences in site characteristics, study design, and timing of sampling in the two studies. The study sites sampled by Apprill and Rappè (2011) were substantially more exposed than our site. At our study site we observed extremely low and variable flow rates (<5 cm/s: Fig. 2), indicating the absence of tidal flushing in the lagoon; flushing rates could well have been higher at the sites occupied by Apprill and Rappe, who did not quantify flushing rates as part of their study. In addition, the timing of the two studies relative to the spawning season was different, and this difference in timing could play a role in the contrasting responses observed. Significant variability in release of spawning material has been observed for *Montipora capitata* between successive months within the same year, with earlier months releasing a larger quantity of spawn material than later months (Padilla-Gamiño and Gates, 2012). Our study was performed in June, whereas the Apprill and Rappè (2011) study was performed in July. Thus, it may be that a larger quantity of spawn material was released during our sampling, relative to that of Apprill and Rappè (2011). These differences emphasize the variability in biogeochemical response that can be observed in the same region as a function of sampling on different spatial and temporal scales.

6. Summary and conclusions

We observed: (1) a change in the isotopic signatures of coral colonies after a spawning event; (2) rapid turnover of SDOM within the water column and enhanced deposition of POM to the sediment surface; (3) enhanced sediment efflux of NH_4^+ after spawning that provided sufficient nutrients to fuel a phytoplankton bloom event; (4) drawdown of dissolved water column nutrient inventories after spawning that coincide with enhanced phytoplankton biomass, and (5) diatom dominance within the bloom, which was verified by both pigment concentrations and $Si(OH)_4$ drawdown. These observations, when taken together, are consistent with a SDOM-triggered phytoplankton bloom. We note that the timing and magnitude of the SDOM-triggered bloom event in Kane'ohe Bay is consistent with previous research that has documented phytoplankton blooms triggered by episodic nutrient loading to Kane'ohe Bay by storm-driven river input, and by coral spawning events in other systems.

Substantial differences exist in the post-spawn behavior of water column nutrients in the GBR, as contrasted with our study site in Kane'ohe Bay, which highlight the regional variations in nutrient recycling patterns that can occur in different systems. Pelagic and benthic biogeochemical responses associated with SDOM will vary between regions depending upon a number of factors, including: (1) the biochemical composition of released gametes, (2) the magnitude of the spawning event and, in particular, how many species and/or individuals participate in the event, (3) the residence time of SDOM in the water column, which will be influenced by weather, currents, successful fertilization of eggs, and predation intensity, and (4) SDOM recycling and removal processes that may be particular to each environment. Thus, organic matter from coral spawning can have important effects on the metabolism and functioning of the reef ecosystem. Questions remain as to how the intensity and temporal and spatial variation of spawning events interact with the environment to affect reef biogeochemistry. Answers to these questions will enable better prediction of the effects of nutrient loading on reef ecosystems.

Acknowledgments

Jeff Sevadjian supplied support with ADCP data acquisition and presentation, which we gratefully acknowledge. We thank Craig Glenn for access to his coulometer. We are grateful to Danielle Hull, Christine Pequignet, Pablo Quiroga and numerous volunteers who assisted with instrument placement, field preparations, sample collection and laboratory analyses. Thanks to the Point Lab at HIMB and K. Rodgers for her assistance obtaining records from the meteorological station. This paper is funded in part by a grant/cooperative agreement from the National Oceanic and Atmospheric Administration, Project R/CR-18PD, which is sponsored by the University of Hawaii Sea Grant College Program, SOEST, under Institutional Grant No. NA05OAR4171048 from NOAA Office of Sea

Grant, Department of Commerce. JLPG was supported by a CONACYT Graduate Research Fellowship, the World Bank CRTR program and C-MORE. RAB was partially sponsored by NSF-OCE550851 The views expressed herein are those of the author(s) and do not necessarily reflect the views of NOAA, NSF or any of the sub-agencies. UNIHI-SEAGRANT-JC-08-42. This is SOEST contribution number 9007 and HIMB contribution number 1566.

References

Alamaru, A., Loya, Y., Brokovich, E., Yam, R., Shemesh, A., 2009a. Carbon and nitrogen utilization in two species of Red Sea corals along a depth gradient: Insights from stable isotope analysis of total organic material and lipids. Geochim. Cosmochim. Acta 73, 5333–5342.

Apprill, A., Rappè, M.S., 2011. Response of the microbial community to coral spawning in lagoon and reef flat environments of Hawaii, USA. Aquat. Microbial. Ecol. 62, 251–266.

Arrigo, K.R., 2005. Marine microorganisms and global nutrient cycles. Nature 437, 349–355.

Aspila, K.I., Agemian, H., Chau, A.S.Y., 1976. A semi-automated method for the determination of inorganic, organic and total phosphate in sediments. Analyst 101, 187–197.

Baird, A.H., Guest, J.R., Willis, B.L., 2009. Systematic and biogeographical patterns in the reproductive biology of scleractinian corals. Annu. Rev. Ecol. Evol. Syst. 40, 551–571.

Baird, A.H., Pratchett, M.S., Gibson, D.J., Koziumi, N., Marquis, C.P., 2001. Variable palatability of coral eggs to a planktivorous fish. Mar. Freshw. Res. 52, 865–868.

Bidigare, R.R., van Heukelem, L., Trees, C.C., 2005. Analysis of algal pigments by high-performance liquid chromatography. In: Andersen, R. (Ed.), Algal Culturing Techniques. Academic Press, pp. 327–344.

Bodin, N., L.L.h., F., H, C., 2007. Effect of lipid removal on carbon and nitrogen stable isotope ratios in crustacean tissues. J. Exp. Mar. Biol. Ecol. 341, 168–175.

Boudreau, B.P., 1997. Diagenetic Models and Their Implementation, first ed. Springer.

Bray, J.T., Bricker, O.P., Troup, B.N., 1973. Phosphate in interstitial waters of anoxic sediments: oxidation effects during sampling procedure. Science 180, 1362–1364.

Eyre, B.D., Ferguson, J.P., 2006. Impact of a flood event on benthic and pelagic coupling in a sub-tropical east Australian estuary (Brunswick). Estuar. Coast. Shelf Sci. 66, 111–112.

Eyre, B.D., Glud, R.N., Patten, N., 2008. Mass coral spawning: a natural large-scale nutrient addition experiment. Limnol. Oceanogr. 53, 997–1013.

Fry, B., 1988. Food web structure on Georges Bank from stable C, N, and S isotopic compositions. Limnol. Oceanogr. 33, 1182–1190.

Furnas, M., Mitchell, A., Skuza, M., Brodie, J., 2005. In the outer 90%: phytoplankton responses to enhanced nutrient availability in the Great Barrier Reef Lagoon. Mar. Pollut. Bull. 51, 253–263.

Glud, R.N., Eyre, B.D., Patten, N., 2008. Biogeochemical responses to mass coral spawning at the Great Barrier Reef: effects on respiration and primary production. Limnol. Oceanogr. 53, 1014–1024.

Goni, M.A., 1997. 32. Record of terrestrial organic matter composition in Amazon fan sediments. In: Flood, R.D., Piper, D.J.W., Peterson, L.C. (Eds.), Proceedings of the Ocean Drilling Program, Scientisif Results.

Grasshoff, K., Ehrhardt, M., Kremling, K. (Eds.), 1983. Methods of Seawater Analysis, second ed. Verlag Chemie, Weinheim.

Grasshoff, R., Ehrhardt, M., Kremling, K. (Eds.), 1976. Methods of Seawater Analysis. Verlag Chemie, pp. 150–157.

Grottoli, A.G., Rodrigues, L.J., 2011. Bleached *Porites compressa* and *Montipora capitata* corals catabolise δ^{13}C-enriched lipids. Coral Reefs 30 (3), 687–692.

Grottoli, A.G., Rodrigues, L.J., Juarez, C., 2004. Lipids and stable carbon isotopes in two species of Hawaiian corals, *Porites compressa* and *Montipora verrucosa*, following a bleaching event. Mar. Biol. 145, 621–631.

Grottoli, A.G., Wellington, G.M., 1999. Effect of light and zooplankton on skeletal delta C-13 values in the eastern Pacific corals *Pavona clavus* and *Pavona gigantea*. Coral Reefs 18, 29–41.

Guest, J., 2008. How reefs respond to mass coral spawning. Science 320, 621–623.

Harrison, P.L., Wallace, C.C., 1990. Reproduction, dispersal and recruitment of scleractinian corals. In: Dubinsky, Z. (Ed.), Ecosystems of the World, Coral Reefs. Elsevier Science Publishers B.V., pp. 133–207.

Healey, F.P., Hendzel, L.L., 1980. Physiological indicators of nutrient deficiency in lake phytoplankton. Can. J. Fish. Aquat. Sci. 37, 442–453.

Hecky, R.E., Kilham, P., 1988. Nutrient limitation of phytoplankton in freshwater and marine environments: a review of recent evidence on the effects of enrichment. Limnol. Oceanogr. 33, 796–822.

Hedges, J.I., Parker, P.L., 1976. Land-derived organic matter in surface sediments from the Gulf of Mexico. Geochim. Cosmochim. Acta 40, 1019–1029.

Jokiel, P.L., Brown, E.K., Friedlander, A., Rodgers, S.K., Smith, W.R., 2004. Hawaii Coral Reef Assessment and Monitoring Program: spatial patterns and temporal dynamics in reef coral communities. Pacific Sci. 58, 145–158.

Krall, P., Slomp, C.P., Forster, A., Kuypers, M.M.M., Sluijs, A., 2009. Pyrite oxidation during sample storage determines phosphorus fractionation in carbonate-poor anoxic sediments. Geochim. Cosmochim. Acta 73, 3277–3290.

Laws, E.A., Allen, C.B., 1996. Water quality in a subtropical embayment more than a decade after sewage discharges. Pacific Sci. 50, 194–210.

Maier, C., Weinbauer, M.G., Patzoid, J., 2010. Stable isotopes reveal limitations in C and N assimilation in the Caribbean reef corals *Madracis aurentenra, M. carmabi* and *M. formosa*. Mar. Ecol. Prog. Ser. 412, 103–112.

Menden-Deuer, S., Lessard, E.J., 2000. Carbon to volume relationships for dinoflagellates, diatoms, and other protist plankton. Limnol. Oceanogr. 45, 569–579.

Monaghan, E., Ruttenberg, K.C., 1999. Dissolved organic phosphorus in the coastal ocean: reassessment of available methods and seasonal phosphorus profiles from the Eel River Shelf. Limnol. Oceanogr. 44, 1702–1714.

Padilla-Gamiño, J.L., Bidigare, R., Barshis, D.J., Alamaru, A., Hédouin, L., Hernández-Pech, X., Kandel, F., Leon Soon, S., Roth, M.S., Rodrigues, L.J., Grottoli, A.G., Portocarrero, C., Wagenhauser, S., Buttler, F., Gates, R.D., 2013. Are all eggs created equal? A case study from the Hawaiian reef building coral *Montipora capitata*. Coral Reefs 32 (1), 137–152.

Padilla-Gamiño, J.L., Gates, R.D., 2012. Spawning dynamics in the Hawaiian reef-building coral *Montipora capitata*. Mar. Ecol. Prog. Ser. 449, 145–160.

Padilla-Gamiño, J.L., Weatherby, T., Waller, R.G., Gates, R.D., 2011. Formation and structural organization of the egg-sperm bundle of the scleractinian coral *Montipora capitata*. Coral Reefs 30, 371–380.

Pratchett, M.S., Gust, N., Goby, G., Klanten, S.O., 2001. Consumption of coral propagules represents a significant trophic link between corals and reef fish. Coral Reefs 20, 13–17.

Ringuet, S., Mackenzie, F.T., 2005. Controls on nutrient and phytoplankton dynamics during normal flow and storm runoff conditions, Southern Kaneohe Bay, Hawaii. Estuaries 28, 327–337.

Rodrigues, L.J., Grottoli, A.G., 2006. Calcification rate and the stable carbon, oxygen, and nitrogen isotopes in the skeleton, host tissue, and zooxanthellae of bleached and recovering Hawaiian corals. Geochim. Cosmochim. Acta 70, 2781–2789.

Rodrigues, L.J., Grottoli, A.G., 2007. Energy reserves and metabolism as indicators of coral recovery from bleaching. Limnol. Oceanogr. 52, 1874–1882.

Simpson, C.J., Cary, J.L., Masini, R.J., 1993. Destruction of corals and other reef animals by coral spawn slicks on Ningaloo Reef, Western Australia. Coral Reefs 12, 185–191.

Silversand, C., Haux, C., 1997. Improved high-performance liquid chromatographic method for the separation and quantification of lipid classes: application to fish lipids. J. Chromatogr. B 703, 7–14.

Sokal, R.R., Rohlf, F.J., 1994. Biometry, third ed. W.H. Freeman, New York.

Stimson, J., Larned, S.T., 2000. Nitrogen efflux from the sediments of a subtropical bay and the potential contribution to macroalgal nutrient requirements. J. Exp. Mar. Biol. Ecol. 252, 159–180.

Szmant, A.M., 2002. Nutrient enrichment on coral reefs: Is it a major cause of coral reef decline? Estuaries 25, 743–766.

Wallace, C.C., 1985. Reproduction, recruitment and fragmentation in nine sympatric species of the coral genus *Acropora*. Mar. Biol. 88, 217–233.

Westneat, M.W., Resing, J.M., 1988. Predation on coral spawn by planktivorous fish. Coral Reefs 7, 89–92.

Wild, C., Haas, A., Naumann, M., Mayr, C., el-Zibday, M., 2008. Comparative investigation of organic matter release by corals and benthic reef algae-implications for pelagic and benthic microbial metabolism. In: Proceedings of the 11th Inernational Coral Reef Symposium, Ft. Lauderdale, FL.

Wild, C., Huettel, M., Klueter, A., Kremb, S.G., Rasheed, M.Y.M., Jørgensen, B.B., 2004a. Coral mucus functions as an energy carrier and particle trap in the reef ecosystem. Nature 428, 66–70.

Wild, C., Tollrian, R., Huettel, M., 2004b. Rapid recycling of coral mass-spawning products in permeable reef sediments. Mar. Ecol. Prog. Ser. 271, 159–166.

Wild, C., Woyt, H., Huettel, M., 2005. Influence of coral mucus on nutrient fluxes in carbonate sands. Mar. Ecol. Prog. Ser. 287, 87–98.

Willis, B.L., Babcock, R.C., harrison, P.L., Oliver, J.K., 1985. Patterns in the mass spawning of corals on the Great Barrier Reef from 1981 to 1984. In: Proceedings of the Fifth International Coral Reef Congress, pp. 343–348.